

Article

Not peer-reviewed version

Combined Potential of Quarry Waste Fines and Eggshells for the Hydrothermal Synthesis of Tobermorite at Varying Cement Content

[Shem Quiawan Saldia](#)*, [Hernando P. Bacosa](#), Maria Cristina Vegafria, [Joshua B. Zoleta](#), [Naoki Hiroyoshi](#), Christian Dagunsa Calleno, Wilyneth Sindico Cantong, Ephraim Ibarra, [Maricar Aguilos](#), [Ruben F Amparado](#)

Posted Date: 30 November 2023

doi: 10.20944/preprints202311.1926.v1

Keywords: eggshells; hydrothermal synthesis; quarry waste fines; tobermorite



Preprints.org is a free multidiscipline platform providing preprint service that is dedicated to making early versions of research outputs permanently available and citable. Preprints posted at Preprints.org appear in Web of Science, Crossref, Google Scholar, Scilit, Europe PMC.

Copyright: This is an open access article distributed under the Creative Commons Attribution License which permits unrestricted use, distribution, and reproduction in any medium, provided the original work is properly cited.

Article

Combined Potential of Quarry Waste Fines and Eggshells for the Hydrothermal Synthesis of Tobermorite at Varying Cement Content

Shem Saldia ^{1,*}, Hernando Bacosa ¹, Maria Cristina Vegafria ³, Joshua Zoleta ^{3,4}, Naoki Hiroyoshi ⁴, Christian Calleno ¹, Wilyneth Cantong ¹, Ephraim Ibarra ³, Maricar Aguilos ⁵ and Ruben Amparado, Jr. ^{1,2}

¹ Environmental Science Graduate Program, College of Science and Mathematics, Mindanao State University – Iligan Institute of Technology, Iligan City, Lanao del Norte 9200, Philippines

² Laboratory of Terrestrial Biodiversity, Premier Research Institute of Science and Mathematics (PRISM), Mindanao State University – Iligan Institute of Technology, Iligan City 9200, Philippines

³ College of Engineering and Technology, Mindanao State University – Iligan Institute of Technology, Iligan City, Lanao del Norte 9200, Philippines

⁴ Division of Sustainable Engineering, Chemical Resources Laboratory, Hokkaido University, Sapporo 060 - 0808, Japan

⁵ Department of Forestry and Environmental Resources, North Carolina State University, Raleigh, NC27695, USA

* Correspondence: shem.saldia@g.msuiit.edu.ph; Iligan City, Lanao del Norte 9200, Philippines

Abstract: Quarry waste fines and eggshells are unavoidable wastes which relentlessly contribute to environmental load and pollution. Although a number of studies have suggested various methods for recycling, these wastes remain underutilized due to some technical constraints. In addition, no study has yet been explored on the possibility of combining quarry waste fines (QWF) and eggshell powder (ESP) for tobermorite synthesis. Tobermorite is the main component which primarily provides strength to the autoclaved aerated concrete products. For this purpose, this study seeks to evaluate the potential of QWF- ESP mix at 10%, 15% and 20% amounts of cement, respectively. The XRF, XRD, and TGA-DTA techniques were used to characterize the waste materials while physical and mechanical property tests and XRD analysis were performed on the autoclaved samples. It was found that QWF contains 53.77% SiO₂, while ESP contains 97.8% CaO which are key components for tobermorite synthesis. This study also revealed that the mixture with only 10% cement has the highest compressive strength among the QWF-ESP samples. Furthermore, the formation of tobermorite in the samples was confirmed through XRD analysis. Hence, the hydrothermal curing of QWF –ESP can be further developed to produce functional tobermorite – bearing materials.

Keywords: eggshells; hydrothermal synthesis; quarry waste fines; tobermorite

1. Introduction

Huge amounts of quarry by-products are generated globally mostly from the production of crushed stone or coarse aggregate. These quarry by-products, also known as ‘quarry wastes’ contain considerable amounts of fine particles that exhibit variable composition of minerals. In general, quarry waste consists of different material types invariably known as “quarry fines”, “quarry dust”, “stone by-products”, “recycled aggregates”, “quarry powder wastes”, and so forth [1–3]. Quarry dust is considered a residue after rock crushing and screening to form particles less than 75 µm, consisting of silt, clay, and non-quartz particles. This makes the quarry industry unsustainable since large amounts of these fine materials are produced, which is about 20% to 25 % of the total output of rock processing, which is considered unmarketable and is generally disposed of in landfills [4–6].

Aside from the sustainability issues within the extractive industries, quarry waste fines pose environmental and social impacts, especially at high proportions of extremely fine particles as these are prone to mobilization under the action of gravity and wind. Consequently, these dust emissions pose health risks to workers and surrounding communities. If not properly managed, these dusts may also change native soil properties, and possibly destroy vegetation [2,7]. In addition, quarry dust can cause water contamination and further affects communities when uncontrolled dust finds its way into water sources making water unpleasant for consumption[8–10].

As a response, many researchers from different countries have been exploring the potential uses of quarry by-products. Most of the proposed recycling methods are for structural purposes such as building materials, road development, aggregates, bricks, and tiles. Specifically, quarry fines are applied as partial replacement to natural sand or river sand in the production of various types of concrete. The amount of substitution varies from the chemical and mineralogical properties of different types and sources of quarry wastes. Based on the majority of the studies, 40% to 50% replacement of sand with quarry wastes is the optimal range which has no harmful effect on the concrete's strength and durability[3,11,12]. However, some studies found that a high proportion of fine particles and the presence of other elements in quarry waste have negative effects on the properties (i.e. cohesive property, workability, density, and permeability) of concrete [13,14].

In addition to quarry waste fines, another type of waste that has not been adequately explored as potential raw material for tobermorite synthesis is eggshell powder (ESP). According to some studies, ESP can be employed as a replacement for cement which can be incorporated in concrete, cement mortar, and brick. Other applications of ESP include the following: an additive in bio-ceramics, alkali-activated binder, calcium source, solid catalyst for biodiesel production, soil stabilizer and an additive in bone cement and red wall tiles [15–20]. Based on these findings, ESP is suitable for structural systems since it contains high amounts of calcium, which can be combined with pozzolanic materials. It is also reported that mechanical properties are improved by using eggshell powder. However, some studies reported a reduction of strength when cement is replaced with high percentages of ESP, especially above 10% [21–23].

To sum them up, quarry waste fines (QWF) and eggshell powder (ESP) have been found to have potential by many researchers. However, the recyclability of these materials still has some constraints. Based on the aforementioned published studies, QWF and ESP are limited as partial replacements or substitute materials. At this point, most studies do not recommend using these wastes as the primary raw materials for a product. Aside from that, no research had yet been reported that eggshells can be paired with quarry waste fines found in Mandulog Iligan City, Philippines, specifically to produce a blended formulation for the synthesis of tobermorite.

Currently, the QWF from Mandulog Iligan City has not been thoroughly explored in terms of its recycling potential. Hence, this study seeks to evaluate the characteristics of QWF sourced from Iligan City, along with ESP, and investigate their reaction under high-pressure steam curing method, known as autoclaving or hydrothermal treatment. During this hydrothermal curing, products are strengthened due to the complex reactions affecting the calcium-silicate-hydrate (CSH) phase leading to the formation of tobermorite. Furthermore, the hydrothermal process contributes to the high utilization of solid wastes because of the stimulation of mineral activity, for this reason, various industrial solid wastes can be used for the production of tobermorite-bearing products like AAC [24–27]. Likewise, this study examined the presence of tobermorite mineral since it is considered the main reaction product during the hydrothermal curing process which plays a major role in the structural integrity and strength of the product [28–31].

This study aims to investigate the suitability of QWF and ESP as raw materials for the hydrothermal synthesis of tobermorite. Specifically, this study intends to (1) evaluate the chemical and mineralogical properties of the raw materials; (2) determine the physical and mechanical properties of the autoclaved samples, and (3) determine the presence of tobermorite in the autoclaved samples (at 10%, 15%, and 20% OPC, respectively). The use of additives and pore formers such as gypsum and aluminum powder is not included since this study concerns only the reaction between QWF and ESP and this serves as preliminary research towards the development of AAC using the

aforementioned waste materials. Additionally, only OPC was added which acts as the binder in the sample-forming process, and was limited only to three variations - 10%, 15%, and 20%, respectively. This was carried out in order to evaluate the dependability of QWF-ESP mix with cement. Furthermore, only a Ca/Si ratio of 0.80 was followed in the mixture preparation of QWF-ESP samples [32–34]. Meanwhile, the hydrothermal conditions were fixed at 180 °C for 6 hours [25,26,35–37].

The research presents new possible recycling routes for QWF and ESP which would later contribute to the reduction of environmental load and waste management costs in quarry industries, agriculture, and commercial sectors. Furthermore, this study provides additional insights into the potential use of QWF and ESP as possible starting materials for the synthesis of tobermorite for the future development of autoclave concrete products. In effect, such wastes may be converted into valuable resources and may reduce the demand for raw materials especially river sand and limestone in the future.

2. Materials and Methods

2.1. Raw Material Preparation

This study utilized QWF which was sourced from a river sand quarry site in Mandulog Iligan City, Philippines. In the preparation of the QWF, foreign materials were removed and discarded by sieving 2 kilograms of QWF on a size 20-mesh sieve (840 microns). The screened QWF was then wet milled until a uniform particle size distribution with a fineness of ≤ 75 microns (passing 200-mesh sieve) was achieved [38]. Since QWF is already composed of fine materials, this process only took 3 hours for uniform particle size distribution to be attained. Lastly, the wet milled QWF was oven-dried for at least 4 hours at 110 °C and pulverized.

For the ESP preparation, the collected eggshells were washed thoroughly with water and were then oven-dried for 4 hours at 110 °C. Similar to the quarry waste fines, this study used ESP of particle size ≤ 75 microns [38]. The dried eggshells were milled for at least 5 hours using a porcelain ball mill and screened using a 200-mesh sieve (75 microns) to form finer ESP. Afterwards, the ESP was subjected to pre-treatment which is the calcination process to remove volatile substances and purify the material. This procedure was done by subjecting ESP at 1000°C in a firing furnace [39].

2.2. Raw Material Characterization

X-ray fluorescence analysis (XRF) and X-ray diffraction analysis (XRD) were carried out to determine the chemical composition and mineralogical characteristics of the raw materials that were used for the formulation of the QWF-ESP mix. Approximately 15 grams of powdered sample were prepared for each of the aforementioned analyses. The analyses were carried out via X-ray fluorescence spectroscopy (XRF, EDXL300, Rigaku Corporation, Tokyo, Japan) and X-ray diffraction spectroscopy (XRD, MultiFlex, Rigaku Corporation, Tokyo, Japan). For the XRD, the sample was placed in a platinum sample holder and analyzed at a heating rate of 2°C/min. In addition, the Thermogravimetric Analysis and Differential Thermal Analysis (TGA–DTA) were performed on the raw materials to determine the mass loss and microstructural changes, as well as to identify minerals and hydrates, thus were used to complement the XRD [40–42]. In the TGA–DTA procedure, approximately 70 mg of sample was required which was placed on an aluminum crucible, and subjected to a heating rate of 10°C/min for up to 1000 °C in an oxygen atmosphere.

2.3. Sample Preparation

The samples were produced using QWF and ESP with the forming binder OPC following a Ca/Si ratio of 0.8 in the formulation and mixture preparation [32–34]. Afterwards, water was added to these materials following a 0.70 water-solid ratio and was mixed thoroughly to form a slurry consistency. The slurry was then poured and cast into the cubic mold. After the cast mixture was hardened, it was de-molded and autoclaved at 180 °C for 6 hours [25,26,35–37]. The control sample used was formulated with the traditional raw materials, lime and silica with only 10% OPC while the Ca/Si ratio, water-solid ratio, and autoclaving conditions are consistent with the QWF-ESP samples.

2.4. Determination of Physical and Mechanical Properties

The physical and mechanical properties which include the bulk density, percent water absorption, percent volume of permeable voids and compressive strength tests were performed on the cured samples. Before testing, the samples were prepared through oven drying at 100 to 110°C. The bulk density and water absorption tests were carried out in accordance with ASTM C642-06 guidelines. On the other hand, the compressive strength was determined in accordance with ASTM C1386 -98, 2017 using a Universal Testing Machine (Zhejiang Tugong Instrument Co.,Ltd).

2.5. Determination of Phase Composition of the Autoclaved Samples

X-ray diffraction analysis (XRD) was carried out on the autoclaved samples to determine the presence of the tobermorite and other mineral phases as the resulting products of the hydrothermal reaction between QWF and ESP, in comparison with the control sample (lime and silica). This procedure required the autoclaved sample to be crushed and pulverized using a mortar. The analyses were carried out via X-ray diffraction spectroscopy (XRD, MultiFlex, Rigaku Corporation, Tokyo, Japan).

3. Results and Discussion

3.1. Raw Material Characterization Results

3.1.1. X-Ray Fluorescence Analysis (XRF)

The major chemical/oxide components of the QWF and ESP which were determined by the X-ray fluorescence analysis are shown in Table 1.

Table 1. Chemical compositions of QWF and ESP.

Chemical Composition (Oxides)	QWF (%weight)	ESP (%weight)
SiO ₂	53.77	0.41
CaO	8.89	97.80
Al ₂ O ₃	20.07	0.50
MgO	3.56	-
Fe ₂ O ₃	10.90	0.49
K ₂ O	1.26	0.36
P ₂ O ₅	0.21	0.33
MnO	0.19	-
TiO ₂	0.85	0.01
V ₂ O ₅	0.10	-
CuO	0.02	0.01
ZnO	0.02	-
SO ₃	0.13	0.57

The QWF from Mandulog, Iligan City contains silicon dioxide (SiO₂) as the highest amount, followed by alumina (Al₂O₃), iron oxide (Fe₂O₃) and calcium oxide (CaO), respectively (Table 1). Reported QWF chemical compositions from previous works agree with this result of which most QWF or quarry dust materials consist mainly of the aforementioned oxides with SiO₂ being the highest ranging approximately from 47% to 63% [11,43–45]. The amount of SiO₂ in QWF is also almost similar to the amount of SiO₂ in Class F fly ashes from different regions or countries ranging around 46% to 59% as reported in the literature [38,46–49]. On the other hand, ESP has a high calcium oxide content (CaO) of up to 97.8%. However, the oxide, CaO, is the product of the thermal decomposition of the eggshell [50–52]. Eggshells are almost entirely composed of calcium carbonate (CaCO₃) up to about 95% in normal cases [50,53]. This compound, however, cannot be determined in the XRF analysis. Hence, XRD analysis was carried out to confirm the CaCO₃ phase.

3.1.2. X-Ray Diffraction Analysis (XRD)

X-ray diffraction (XRD) analysis was employed on each sample in order to complement the result of XRF analysis by identifying their mineral phase composition. The X-ray diffraction patterns of QWF and ESP are shown in Figures 1 and 2, respectively.

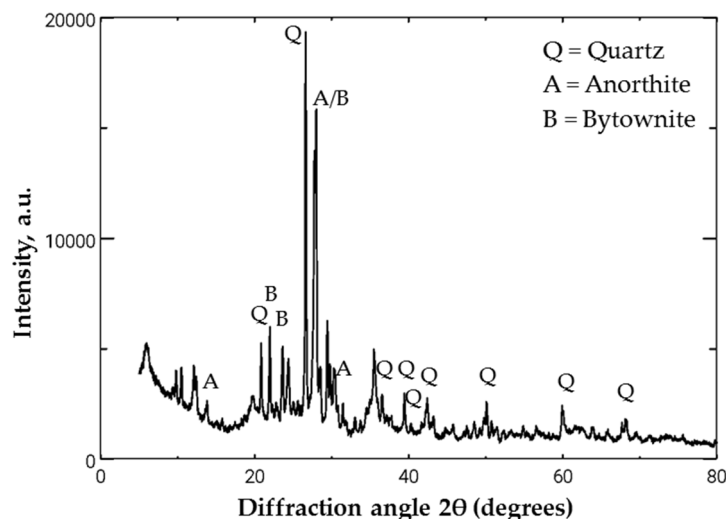


Figure 1. X-Ray Diffraction Pattern of the QWF.

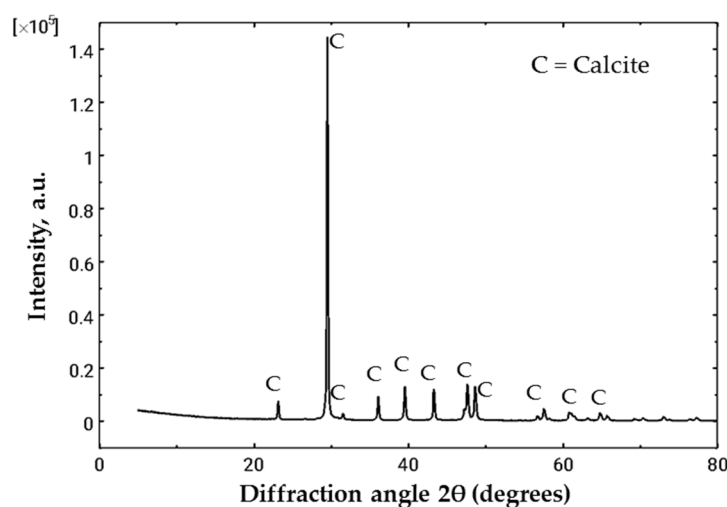


Figure 2. X-Ray Diffraction Pattern of the ESP.

The X-ray diffraction pattern of QWF displays the major phase composition of the material including, anorthite ($\text{Al}_2\text{CaO}_8\text{Si}_2$), bytownite ($\text{Al}_{7.76}\text{Ca}_{3.44}\text{Na}_{0.56}\text{O}_{32}\text{Si}_{8.24}$) and quartz (SiO_2). This implies that SiO_2 in QWF occurs in different mineral forms either (1) as part of anorthite and bytownite or (2) as a crystalline form of SiO_2 known as quartz. However, this material differs from sand in terms of mineral composition. Beach sand for example, reportedly contains more than 72% SiO_2 mostly in the form of quartz. In other words, QWF is composed of more diverse minerals compared to sand. Furthermore, the XRD result agrees with several published works that it is a normal characteristic for quarry fines to contain not only quartz but also other minerals, with similar characteristics to that of mine tailings [11,43,54].

Nevertheless, some standards of tobermorite-containing products like AAC do not require raw material specifications which allows innovation including the use of various silica-rich industrial by-products such as bottom ash, fly ash, blast furnace slag, copper tailing, etc. [55–57]. It was previously mentioned that the amount of SiO_2 in QWF is comparable to fly ash and its mineral phase composition

is similar to mine tailings [58–62]. Hence, this would imply that QWF could also be a promising raw material for the synthesis of tobermorite and later for the fabrication of autoclaved concrete products.

The XRD pattern of ESP is shown in Figure. 2 which shows that its main mineral composition is calcium carbonate, also known as 'calcite' (CaCO_3). This result is consistent with XRF analysis chemical composition results (Table 1) of which ESP consists of up to 97.8% of calcareous material. However, XRF does not reflect carbonates, thus CaO (calcium oxide) is reported. It is in the XRD result, that the true structure of the material is shown as CaCO_3 . Since ESP has a similar composition to limestone, this could also be used as a source of calcium for the synthesis of tobermorite. Materials containing CaCO_3 such as limestone and shells have been used to produce CaO quicklime which is a white, caustic, alkaline, crystalline powder with an array of industrial applications. Limestone, specifically, is one of the most common starting materials in making aerated mixes along with ground slate, also called lime formula [30,51,57].

3.1.3. Thermogravimetric Analysis and Differential Thermal Analysis (TGA-DTA)

The superimposed TGA and DTA curves of QWF are presented in Figure 3. Based on the TGA data, the total mass loss of QWF was -7.2 mg which is equivalent to 10.26% mass loss at 1000°C. Meanwhile, the DTA curve displays an endothermic drop at 98.57°C which is attributed to the loss of surface water and dehydroxylation. Exothermic peaks are also observed at approximately 322.5°C, 758.49°C, and 811.85°C, respectively. The possible reasons for the occurrence of these peaks are due to the chemical and physical changes in QWF including the removal of organic components, decomposition of carbonates and hydroxyls, elimination of water from the interlamellar spaces and the formation of new mineral phases. These results have been validated by some published works on the thermal analysis conducted on some siliceous byproduct-based materials, of which endothermic and exothermic peaks occur at nearly similar temperature levels [63,64]. The DTA results complement and further validate the results of the XRD analysis which implies that QWF is made up of variable mineral composition based on the material's behavior at different temperature levels [65–67].

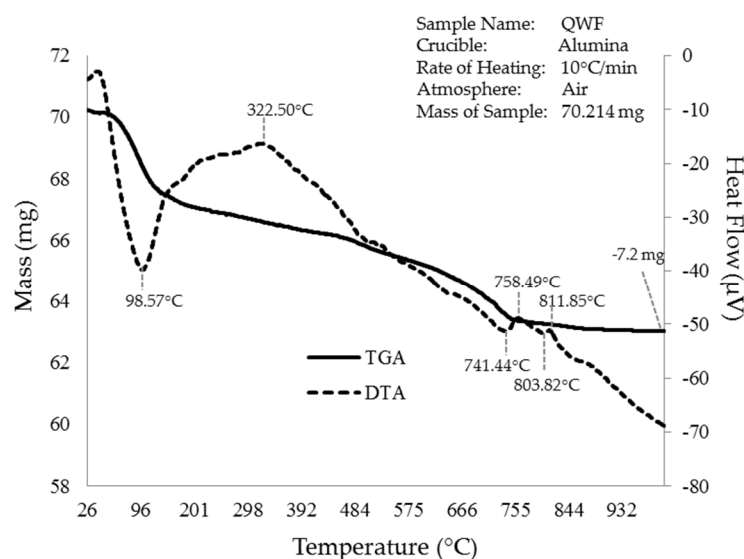


Figure 3. Thermogravimetric analysis and differential thermal analysis (TGA-DTA) graphs of the QWF.

Figure 4 displays the TGA-DTA curves of the ESP raw material which is primarily composed of CaCO_3 . Based on the TGA result, the total mass loss of ESP is approximately -34.0 mg which corresponds to 48.5% mass loss. On the other hand, the DTA curve shows a wide endothermic drop at 75.11°C due to the evaporation of surface water or physically absorbed water. Moreover, an exothermic peak occurred at 348.22°C due to the degradation of organic materials. These results are

supported by literature stating that the decomposition of volatile materials such as moisture or surface water and organic compounds occurs at the range of 30°C to 400°C. The loss of organic compounds is primarily due to the removal of a membrane adhered to the eggshell. This membrane consists of carbohydrates and proteins which are rich in organic matter [68–70]. Another endothermic fluctuation along with a sharp drop of mass of approximately -24.76 mg is observed at 849.82°C which indicates the decomposition of CaCO_3 . These results agree with the findings of existing studies in which the TGA-DTA patterns appear relatively similar to this current study indicating that all major reactions took place in and around the same temperature levels [67,71,72]. Similar to the TGA-DTA analysis of QWF, this result is important since this further confirms the mineral composition of ESP, in this case, the CaCO_3 . This material therefore, needs to be calcined to produce CaO (also known as eggshell lime) and enhance its chemical properties [39,73,74].

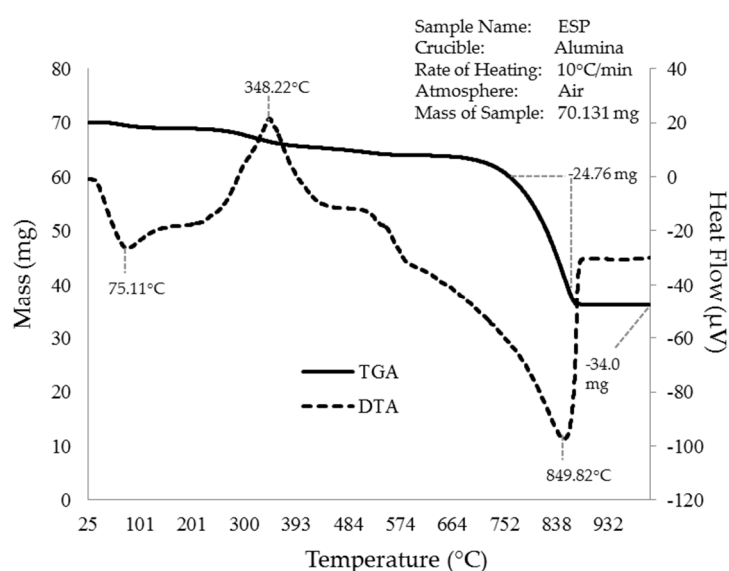


Figure 4. Thermogravimetric analysis and differential thermal analysis (TGA-DTA) graphs of the ESP.

3.2. Physical and Mechanical Properties of the Cured Samples

The bulk density, water absorption and volume of permeable void spaces are key parameters that predict the performance and durability of the concrete or cement-based materials. Usually, the bulk density is inversely related to porosity while water absorption is linearly related to porosity. Water absorption is a descriptor of the material's durability since water can facilitate the transport of the most aggressive ions that may penetrate cement-based materials [75,76]. In this case, the bulk density, water absorption and volume of permeable voids were determined to evaluate the physical properties of the samples and the results are shown in Figure 5.

Trends in the bulk densities, water absorption and volume of permeable voids are observed among samples QWF-ESP10, QWF-ESP15 and QWF-ESP20, respectively. The results show that the OPC amount has significant effects ($p < 0.05$) on the cured physical properties of the blended QWF and ESP. In the QWF-ESP mix, the higher the OPC, the higher the percent water absorption and percent volume of permeable voids. In contrast, the higher the OPC, the lower the bulk density. This further suggests that the QWF-ESP10 which has the lowest percent water absorption and highest bulk density is the least porous among QWF-ESP samples. Moreover, the physical characteristics of LS10 are clearly different from the QWF-ESP samples as they exhibit the least density, yet have low water absorption and permeable voids. This implies that the replacement of lime-silica mix by blended waste materials QWF-ESP has significant effects on the physical properties ($p < 0.05$).

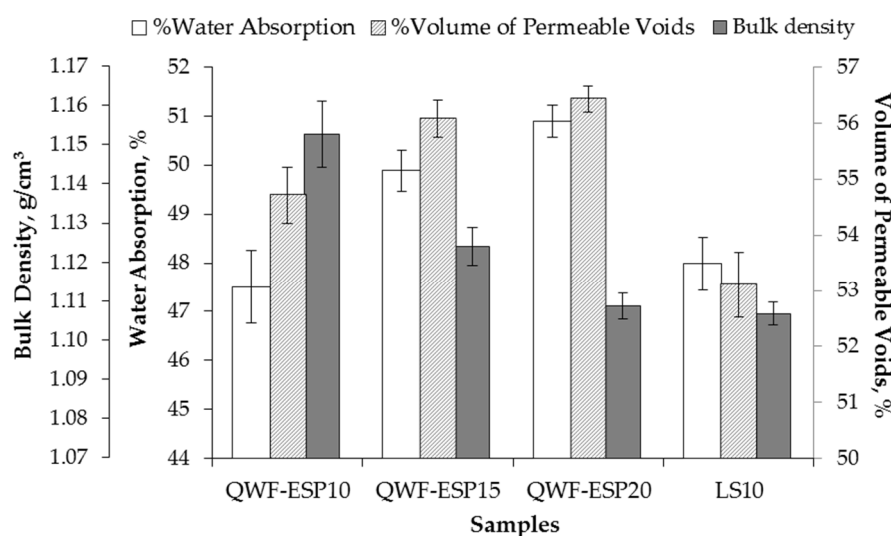


Figure 5. Bulk densities, percent water absorption and percent volume of permeable void spaces of the samples.

The porosity of the autoclaved product is the main determining factor of the compressive strength. Hence, to further support the physical property test results, the compressive strengths of the samples were determined (displayed in Figure 6). Herein, it can be observed that the different amounts of OPC have significant effects on the compressive strengths of QWF-ESP samples. QWF-ESP10 has higher compressive strength than QWF-ESP15 and QWF-ESP20. This suggests that a lower amount of OPC could produce a stronger autoclaved QWF-ESP product. In addition, the QWF-ESP samples have significantly lower compressive strengths than the reference sample LS10. Yet, the QWF-ESP samples have higher bulk densities compared to LS10 (Figure 5). This could mean that QWF-ESP samples and LS10 have different pore characteristics. LS10 could have thicker pore walls than QWF-ESPs, resulting in higher strength while having a low bulk density [25,26]

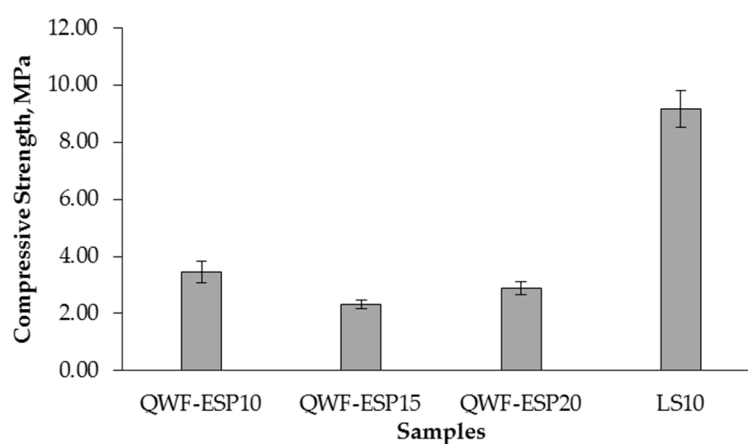


Figure 6. Compressive strengths of the samples.

3.3. Phase Compositions of the Cured Samples

Figure 7 shows the superimposed diffraction patterns of the QWF-ESP cured samples at 10%, 15% and 20% OPC along with the cured lime-silica formulated reference sample (LS10).

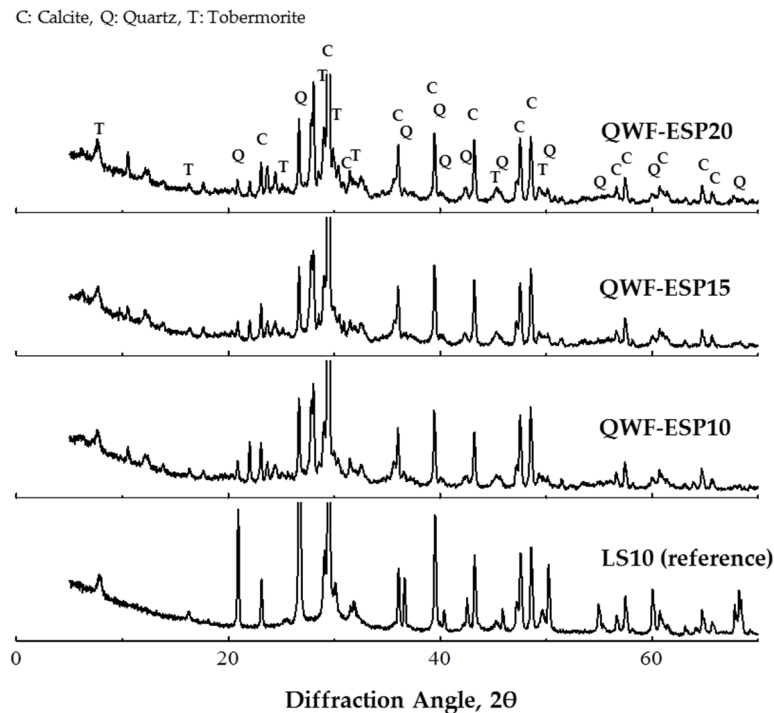


Figure 6. X-Ray Diffraction Patterns of the Cured Samples.

From the XRD results, it was confirmed that tobermorite phases were present in the samples which are represented by visible peaks at diffraction angles around 7.77° (2θ) and 16.20° (2θ), respectively. Several peaks were also found around 26.60° (2θ), 29° to 32° (2θ), 40° to 42° (2θ), and 47° to 51° (2θ), respectively which appear to overlap with other phases like calcite and quartz. The presence of these low-intensity peaks implies that QWF reacted with ESP to form tobermorite under hydrothermal conditions which are somewhat similar to the XRD findings of several published studies [25,26,77,78]. It was also observed that QWF-ESP samples were almost similar to the LS10 control sample in terms of peak intensities. Furthermore, it can be observed that samples QWF-ESP10, QWF-ESP15 and QWF-ESP20, respectively have an almost similar degree of tobermorite crystallinity especially at 7.77° (2θ) and 16.20° (2θ), respectively which suggest that autoclaving a QWF-ESP formulated body can produce tobermorite regardless if it uses 10%, 15% or 20% OPC. In this case, QWF-ESP10 which has the lowest OPC amount is more favorable in terms of reducing starting material usage. In this study, one fundamental question that still remains unanswered while it is beyond its scope, is “What specific steam curing conditions and optimum mix design and concentrations of OPC in the QWF-ESP formulation will yield more crystalline-structured tobermorite products as a result of the hydrothermal process?”

4. Implications

As previously stated, the investigation of blended QWF and ESP to form tobermorite and the effects of varied OPC amounts on the properties of the autoclaved samples were the main emphasis of this study. Tobermorite is responsible for the strength of autoclaved aerated concrete (AAC). According to the literature, AAC is one of the confirmed green structures that permits the use of many raw material types in its manufacture. Some of these substitute materials are effective in reducing cement consumption in the production of AAC, thus leading to a reduction of greenhouse gases [79,80]. The characterization of QWF and ESP, in this study, revealed that these waste materials contain the key components for tobermorite synthesis such as SiO_2 and CaO . Aside from construction applications, tobermorite has been gaining more attention in recent years due to its high utilization value in chemical and mechanical industries, its economy of materials, as well as its potential for environmental cleanup purposes [78,81–83].

In the present work, the tobermorite phase was formed despite the differences in mineralogical characteristics of QWF and ESP from the traditional raw materials (i.e. lime, sand and chemically-grade silica). However, the QWF-ESP samples have lower compressive strengths than the reference sample. Nevertheless, these findings will serve as a starting point for future innovation that will encompass technical challenges associated with exploring the vast potentials of tobermorite and the hydrothermal process to utilize waste by-products for the development of an environmentally sustainable building material.

Furthermore, using QWF as the main source of silica and calcined ESP as the source of lime could potentially conserve sand or silica resources and limestone. QWF is also composed of finer materials than sand. Moreover, QWF is much cheaper compared to commercial chemically-grade silica. Thus, recycling waste by-products like QWF and ESP not only reduces environmental load but also promotes resource efficiency in the building sector. Finally, it should be noted that this is a preliminary study that has been conducted to determine the potential of the mixture of QWF and ESP as possible alternatives to the traditional AAC raw materials (i.e., lime and silica sand) in the synthesis of tobermorite. Understanding the properties of the raw materials in order to determine the appropriate pretreatment method and to optimize their proportions in the mix, as well as considering the concentration of OPC, and hydrothermal curing conditions becomes necessary to come up with a high quantity of crystalline tobermorite. More importantly, this study provides the individual chemical and mineralogical characteristics of QWF and ESP which could be used not only for tobermorite synthesis but for other recycling or waste valorization and solidification strategies (i.e. heavy metal immobilization).

5. Conclusions and Recommendations

In this study, the chemical, mineralogical and physical characteristics of quarry waste fines and eggshells were evaluated. Their suitability to form tobermorite-bearing material with different amounts of OPC binder was also investigated via physical and mechanical property tests and XRD analysis. Using different characterization techniques, the QWF was found to have a considerable amount of silicon dioxide or silica (SiO_2) content. On the other hand, ESP contains high purity CaCO_3 making it a rich source of calcium (Ca) or calcium oxide (CaO). These would imply that QWF and ESP can be used as alternative starting materials for tobermorite synthesis which may be applied in the future for the manufacture of AAC. In addition, the full replacement of traditional lime-silica raw materials by QWF-ESP has significant effects on the physical and mechanical properties of the product. The QWF-ESP with the least amount of OPC has the highest strength among QWF-ESP samples which is favorable for saving raw materials. Furthermore, hydrothermal curing of QWF-ESP-based samples at 180°C for 6 hours was able to produce tobermorite, as confirmed by XRD results. It was found that the tobermorite peaks are visible in the QWF-ESP samples and the peak intensities are closely similar to the lime-silica formulation. Therefore, QWF-ESP with lower OPC can be further developed to produce tobermorite-bearing materials like AAC.

According to the literature, in order to obtain products with ideal properties, crystalline tobermorite should be the main phase formed after hydrothermal treatment [25,26]. Hence, the present work needs further improvement since the QWF-ESP formulations were not sufficient in terms of achieving a comparable strength to the reference sample, suggesting that the amount of tobermorite formed was also insufficient. Nevertheless, since lower OPC had positive effects on the compressive strength, it is highly recommended to conduct a follow-up experiment using the same or lower range of OPC at varying hydrothermal temperatures or curing time to further validate the findings in this study. If this is not possible for the casting method, it is also suggested to explore other forming methods such as semi-dry pressing. Furthermore, it is recommended to vary the mix design and incorporate additives (i.e. gypsum or anhydrite) as possible methods to enhance the properties of the cured product.

Author Contributions: Conceptualization, S.S.; methodology, S.S., C.C. and W.C.; software, J.Z. and N.H.; formal analysis, S.S. and J.Z.; resources, E.I., J.Z. and N.H.; data curation, S.S.; writing—original draft preparation, S.S.; writing—review and editing, R.A., J.Z., H.B., M.C.V. and M.A.; visualization, S.S., J.Z. and R.A.; supervision, R.A., H.B. and M.C.V. All authors have read and agreed to the published version of the manuscript.

Funding: This research received no external funding.

Institutional Review Board Statement: Not applicable.

Informed Consent Statement: Not applicable.

Acknowledgments: The authors are grateful for the overwhelming support of the MSU-IIT Environmental Science Graduate Program, Department of Biological Sciences, and the Hokkaido University, Division of Sustainable Engineering, especially the Chemical Resources Laboratory for the XRF and XRD analysis. Moreover, the authors wish to thank the MSU-IIT Technology Application and Promotion Unit - Ceramic Training Center for sharing their facilities, the Department of Chemical Engineering and Technology for analyzing the samples and providing the TGA-DTA results and the Megatesting Center, Inc. for the compressive strength test. The Department of Science and Technology-Accelerated Science and Technology Human Resources Program (DOST-ASTHRDP) through the DOST-Science Education Institute (DOST-SEI) is gratefully acknowledged for the scholarship and research grants to the first author.

Conflicts of Interest: The authors declare no conflict of interest.

References

1. Borigarla, B.; Buddaha, T.; G, S.K.; Hait, P. Experimental Study on Replacing Sand by M-Sand and Quarry Dust in Rigid Pavements. *Mater Today Proc* **2022**, *60*, 658–667, doi:10.1016/j.matpr.2022.02.265. <https://doi.org/10.1016/j.matpr.2022.02.265>.
2. Singhal, A.; Goel, S.; Sengupta, D. Physicochemical and Elemental Analyses of Sandstone Quarrying Wastes to Assess Their Impact on Soil Properties. *J Environ Manage* **2020**, *271*, 111011, doi:10.1016/j.jenvman.2020.111011. <https://doi.org/10.1016/j.jenvman.2020.111011>.
3. Zhang, Y.; Korkiala-Tanttu, L.K.; Gustavsson, H.; Miksic, A. Assessment for Sustainable Use of Quarry Fines as Pavement Construction Materials: Part I—Description of Basic Quarry Fine Properties. *Materials* **2019**, *12*, 1209, doi:10.3390/ma12081209. <https://doi.org/10.3390/ma12081209>.
4. Mitikie, B.B.; Alemu, Y.L.; Reda, S.G. Utilization of Basaltic Quarry Dust as a Partial Replacement of Cement for Hollow Concrete Block Production. *Int J Concr Struct Mater* **2022**, *16*, 55, doi:10.1186/s40069-022-00546-4. <https://doi.org/10.1186/s40069-022-00546-4>.
5. Pathe, A.K.; Kumar Kushwaha, P.; Thomas, J.M. Review on Performance of Quarry Dust as Fine Aggregate in Concrete. *International Research Journal of Engineering and Technology* **2020**. www.irjet.net.
6. Schankoski, R.A.; de Matos, P.R.; Pilar, R.; Prudêncio, L.R.; Ferron, R.D. Rheological Properties and Surface Finish Quality of Eco-Friendly Self-Compacting Concretes Containing Quarry Waste Powders. *J Clean Prod* **2020**, *257*, 120508, doi:10.1016/j.jclepro.2020.120508. <https://doi.org/10.1016/j.jclepro.2020.120508>.
7. Cheah, C.B.; Lim, J.S.; Ameri, F. Quarry Dust. In *Sustainable Concrete Made with Ashes and Dust from Different Sources*; Elsevier, 2022; pp. 507–543. <https://doi.org/10.1016/B978-0-12-824050-2.00002-4>.
8. Bakamwesiga, H.; Mugisha, W.; Kisira, Y.; Muwanga, A. An Assessment of Air and Water Pollution Accrued from Stone Quarrying in Mukono District, Central Uganda. *Journal of Geoscience and Environment Protection* **2022**, *10*, 25–42, doi:10.4236/gep.2022.105003. <https://doi.org/10.4236/gep.2022.105003>.
9. Dibattista, I.; Camara, A.R.; Molderez, I.; Benassai, E.M.; Palozza, F. Socio-Environmental Impact of Mining Activities in Guinea: The Case of Bauxite Extraction in the Region of Boké. *J Clean Prod* **2023**, *387*, 135720, doi:10.1016/j.jclepro.2022.135720. <https://doi.org/10.1016/j.jclepro.2022.135720>.
10. Githiria, J.M.; Onifade, M. The Impact of Mining on Sustainable Practices and the Traditional Culture of Developing Countries. *J Environ Stud Sci* **2020**, *10*, 394–410, doi:10.1007/s13412-020-00613-w. <https://doi.org/10.1007/s13412-020-00613-w>.
11. AL-Kharabsheh, B.N.; Moafak Arbili, M.; Majdi, A.; Ahmad, J.; Deifalla, A.F.; Hakamy, A.; Majed Alqawasmeh, H. Feasibility Study on Concrete Made with Substitution of Quarry Dust: A Review. *Sustainability* **2022**, *14*, 15304, doi:10.3390/su142215304. <https://doi.org/10.3390/su142215304>.
12. Shyam Prakash, K.; Rao, Ch.H. Study on Compressive Strength of Quarry Dust as Fine Aggregate in Concrete. *Advances in Civil Engineering* **2016**, *2016*, 1–5, doi:10.1155/2016/1742769. <https://doi.org/10.1155/2016/1742769>.

13. Basu, P.; Thomas, B.S.; Gupta, R.C.; Agrawal, V. Properties of Sustainable Self-Compacting Concrete Incorporating Discarded Sandstone Slurry. *J Clean Prod* **2021**, *281*, 125313, doi:10.1016/j.jclepro.2020.125313. <https://doi.org/10.1016/j.jclepro.2020.125313>.
14. Rathore, K.; Agrawal, V.; Nagar, R. Effect of Waste Sandstone Microfines on Mechanical Strength, Abrasion Resistance, and Permeability Properties of Concrete. *Mater Today Proc* **2022**, *61*, 571–578, doi:10.1016/j.matpr.2022.02.299. <https://doi.org/10.1016/j.matpr.2022.02.299>.
15. Amiri, A.; Toufigh, M.M.; Toufigh, V. Recycling and Utilization Assessment of Municipal Solid Waste Materials to Stabilize Aeolian Sand. *KSCE Journal of Civil Engineering* **2023**, *27*, 1042–1053, doi:10.1007/s12205-022-1418-1. <https://doi.org/10.1007/s12205-022-1418-1>.
16. Ferreira, F.A.; Desir, J.M.; Lima, G.E.S. de; Pedroti, L.G.; Franco de Carvalho, J.M.; Lotero, A.; Consoli, N.C. Evaluation of Mechanical and Microstructural Properties of Eggshell Lime/Rice Husk Ash Alkali-Activated Cement. *Constr Build Mater* **2023**, *364*, 129931, doi:10.1016/j.conbuildmat.2022.129931. <https://doi.org/10.1016/j.conbuildmat.2022.129931>.
17. Hasan, M.; Zaini, M.S.I.; Yie, L.S.; Masri, K.A.; Putra Jaya, R.; Hyodo, M.; Winter, M.J. Effect of Optimum Utilization of Silica Fume and Eggshell Ash to the Engineering Properties of Expansive Soil. *Journal of Materials Research and Technology* **2021**, *14*, 1401–1418, doi:10.1016/j.jmrt.2021.07.023. <https://doi.org/10.1016/j.jmrt.2021.07.023>.
18. Sathiparan, N.; Anburuvel, A.; Selvam, V.V. Utilization of Agro-Waste Groundnut Shell and Its Derivatives in Sustainable Construction and Building Materials – A Review. *Journal of Building Engineering* **2023**, *66*, 105866, doi:10.1016/j.job.2023.105866. <https://doi.org/10.1016/j.job.2023.105866>.
19. Sathiparan, N. Utilization Prospects of Eggshell Powder in Sustainable Construction Material – A Review. *Constr Build Mater* **2021**, *293*, 123465, doi:10.1016/j.conbuildmat.2021.123465. <https://doi.org/10.1016/j.conbuildmat.2021.123465>.
20. Ngayakamo, B.; Onwualu, A.P. Recent Advances in Green Processing Technologies for Valorisation of Eggshell Waste for Sustainable Construction Materials. *Heliyon* **2022**, *8*, e09649, doi:10.1016/j.heliyon.2022.e09649. <https://doi.org/10.1016/j.heliyon.2022.e09649>.
21. Hamada, H.M.; Tayeh, B.A.; Al-Attar, A.; Yahaya, F.M.; Muthusamy, K.; Humada, A.M. The Present State of the Use of Eggshell Powder in Concrete: A Review. *Journal of Building Engineering* **2020**, *32*, 101583, doi:10.1016/j.job.2020.101583. <https://doi.org/10.1016/j.job.2020.101583>.
22. Mahmood, L.; Rafiq, S.; Mohammed, A. A Review Study of Eggshell Powder as Cement Replacement in Concrete. *Sulaimani Journal for Engineering Sciences* **2019**, *9*, 25–38, doi:10.17656/sjes.10150. <https://doi.org/10.17656/sjes.10150>.
23. Shcherban', E.M.; Stel'makh, S.A.; Beskopylny, A.N.; Mailyan, L.R.; Meskhi, B.; Varavka, V.; Beskopylny, N.; El'shaeva, D. Enhanced Eco-Friendly Concrete Nano-Change with Eggshell Powder. *Applied Sciences* **2022**, *12*, 6606, doi:10.3390/app12136606. <https://doi.org/10.3390/app12136606>.
24. Abhilasha; Kumar, R.; Lakhani, R.; Mishra, R.K.; Khan, S. Utilization of Solid Waste in the Production of Autoclaved Aerated Concrete and Their Effects on Its Physio-Mechanical and Microstructural Properties: Alternative Sources, Characterization, and Performance Insights. *Int J Concr Struct Mater* **2023**, *17*, 6, doi:10.1186/s40069-022-00569-x. <https://doi.org/10.1186/s40069-022-00569-x>.
25. Shams, T.; Schober, G.; Heinz, D.; Seifert, S. Production of Autoclaved Aerated Concrete with Silica Raw Materials of a Higher Solubility than Quartz Part II: Influence of Autoclaving Temperature. *Constr Build Mater* **2021**, *287*, 123072, doi:10.1016/j.conbuildmat.2021.123072. <https://doi.org/10.1016/j.conbuildmat.2021.123072>.
26. Shams, T.; Schober, G.; Heinz, D.; Seifert, S. Production of Autoclaved Aerated Concrete with Silica Raw Materials of a Higher Solubility than Quartz Part I: Influence of Calcined Diatomaceous Earth. *Constr Build Mater* **2021**, *272*, 122014, doi:10.1016/j.conbuildmat.2020.122014. <https://doi.org/10.1016/j.conbuildmat.2020.122014>.
27. Xu, L.; Sun, Z.; Tang, C.; Yang, K.; Li, B.; Zhang, Y.; Yang, Z.; Wu, K. Mitigation Effect of Accelerators on the Lead–Zinc Tailing Induced Retardation in Autoclaved Concrete. *Constr Build Mater* **2022**, *352*, 128929, doi:10.1016/j.conbuildmat.2022.128929. <https://doi.org/10.1016/j.conbuildmat.2022.128929>.
28. Lam, N.N. Recycling of AAC Waste In The Manufacture of Autoclaved Aerated Concrete In Vietnam. *International Journal of GEOMATE* **2021**, *20*, doi:10.21660/2021.78.j2048. <https://doi.org/10.21660/2021.78.j2048>.

29. Mesecke, K.; Malorny, W.; Warr, L.N. Understanding the Effect of Sulfate Ions on the Hydrothermal Curing of Autoclaved Aerated Concrete. *Cem Concr Res* **2023**, *164*, 107044, doi:10.1016/j.cemconres.2022.107044. <https://doi.org/10.1016/j.cemconres.2022.107044>.
30. Stepien, A.; Dachowski, R.; Piotrowski, J.Z. Insulated Autoclaved Cellular Concretes and Improvement of Their Mechanical and Hydrothermal Properties. In: 2022; pp. 393–419. https://doi.org/10.1007/978-3-030-98693-3_13.
31. Zhou, L.; Ma, B.; Zhou, H.; Zang, J.; Wang, J.; Qian, B.; Luo, Y.; Ren, X.; Xiao, Y.; Hu, Y. Effect of Ca/Si Ratio on the Properties of Steel Slag and Deactivated ZSM-5 Autoclaved Aerated Concrete. *Journal of the Indian Chemical Society* **2023**, *100*, 100853, doi:10.1016/j.jics.2022.100853. <https://doi.org/10.1016/j.jics.2022.100853>.
32. Majdinasab, A.; Yuan, Q. Synthesis of Al-Substituted 11Å Tobermorite Using Waste Glass Cullet: A Study on the Microstructure. *Mater Chem Phys* **2020**, *250*, 123069, doi:10.1016/j.matchemphys.2020.123069. <https://doi.org/10.1016/j.matchemphys.2020.123069>.
33. Malferrari, D.; Bernini, F.; Di Giuseppe, D.; Scognamiglio, V.; Gualtieri, A.F. Al-Substituted Tobermorites: An Effective Cation Exchanger Synthesized from “End-of-Waste” Materials. *ACS Omega* **2022**, *7*, 1694–1702, doi:10.1021/acsomega.1c04193. <https://doi.org/10.1021/acsomega.1c04193>.
34. Schreiner, J.; Goetz-Neunhoeffer, F.; Neubauer, J.; Jansen, D. Hydrothermal Synthesis of 11 Å Tobermorite – Effect of Adding Metakaolin to the Basic Compound. *Appl Clay Sci* **2020**, *185*, 105432, doi:10.1016/j.clay.2019.105432. <https://doi.org/10.1016/j.clay.2019.105432>.
35. Demir, İ.; Ogdu, M.K.; Sevim, O.; Dogan, O. Mechanical and Physical Properties of Autoclaved Aerated Concrete Reinforced Using Carbon Fibre of Different Lengths. *Tehnicki vjesnik - Technical Gazette* **2021**, *28*, doi:10.17559/TV-20200218194755. <https://doi.org/10.17559/TV-20200218194755>.
36. Pan, Y.; Jiang, Y.; Liu, Z.; Xiang, Q.; Gao, C. Effect of Crystallinity on Properties of Autoclaved Aerated Concrete Matrix Materials. *J Phys Conf Ser* **2023**, *2437*, 012040, doi:10.1088/1742-6596/2437/1/012040. <https://doi.org/10.1088/1742-6596/2437/1/012040>.
37. Serdyuk, V.; Rudchenko, D.; Dyuzhilova, N. The Use of Low Clinker Binders in the Production of Autoclaved Aerated Concrete by Cutting Technology. *Eastern-European Journal of Enterprise Technologies* **2020**, *6*, 63–71, doi:10.15587/1729-4061.2020.217308. <https://doi.org/10.15587/1729-4061.2020.217308>.
38. Zhang, Y.; Miksic, A.; Castillo, D.; Korkiala-Tanttu, L. Microstructural Behaviour of Quarry Fines Stabilised with Fly Ash-Based Binder. *Road Materials and Pavement Design* **2022**, *1–14*, doi:10.1080/14680629.2022.2064904. <https://doi.org/10.1080/14680629.2022.2064904>.
39. Nipunika, U.; Jayaneththi, Y.; Sewwandi, G.A. Synthesis of Calcium Oxide Nanoparticles from Waste Eggshells. In Proceedings of the 2022 Moratuwa Engineering Research Conference (MERCon); IEEE, July 27 2022; pp. 1–5. <https://doi.org/10.1109/MERCon55799.2022.9906264>.
40. Akula, P.; Naik, S.R.; Little, D.N. Evaluating the Durability of Lime-Stabilized Soil Mixtures Using Soil Mineralogy and Computational Geochemistry. *Transportation Research Record: Journal of the Transportation Research Board* **2021**, *2675*, 1469–1481, doi:10.1177/03611981211007848. <https://doi.org/10.1177/03611981211007848>.
41. Flegar, M.; Serdar, M.; Londono-Zuluaga, D.; Scrivener, K. Upotreba Termogravimetrijske Analize Kod Karakterizacije Glina Kao Cementnih Dodataka. In Proceedings of the 6th Symposium on Doctoral Studies in Civil Engineering; University of Zagreb Faculty of Civil Engineering, September 10 2019; pp. 153–162. <https://doi.org/10.5592/co/phdsym.2020.12>.
42. Jayasingh, S.; Selvaraj, T. Effect of Natural Herbs on Hydrated Phases of Lime Mortar. *Journal of Architectural Engineering* **2020**, *26*, doi:10.1061/(ASCE)AE.1943-5568.0000420. [https://doi.org/10.1061/\(ASCE\)AE.1943-5568.0000420](https://doi.org/10.1061/(ASCE)AE.1943-5568.0000420).
43. Aliyu, I.; Sulaiman, T.A.; Mohammed, A.; Kaura, J.M. Effect of Sulphuric Acid on the Compressive Strength of Concrete with Quarry Dust as Partial Replacement of Fine Aggregate. *FUDMA Journal of Sciences* **2020**, *4*, 553–559. <https://www.researchgate.net/publication/340455044>.
44. Koganti, S.P.; Chappidi, H.R. Geotechnical Properties of Quarry Dust. *Electronic Journal of Geotechnical Engineering* **2016**, *21*, 2963–2973. <https://www.researchgate.net/publication/303859484>.
45. Taiwo, L.A.; Obianyo, I.I.; Omoniyi, A.O.; Onwualu, A.P.; Soboyejo, A.B.O.; Amu, O.O. Mechanical Behaviour of Composite Produced with Quarry Dust and Rice Husk Ash for Sustainable Building Applications. *Case Studies in Construction Materials* **2022**, *17*, e01157, doi:10.1016/j.cscm.2022.e01157. <https://doi.org/10.1016/j.cscm.2022.e01157>.

46. Abhishek, H.S.; Prashant, S.; Kamath, M. V.; Kumar, M. Fresh Mechanical and Durability Properties of Alkali-Activated Fly Ash-Slag Concrete: A Review. *Innovative Infrastructure Solutions* **2022**, *7*, 116, doi:10.1007/s41062-021-00711-w. <https://doi.org/10.1007/s41062-021-00711-w>.
47. Holanda, J.N.F. The Properties and Durability of Clay Fly Ash-Based Fired Masonry Bricks. In *Eco-Efficient Masonry Bricks and Blocks*; Elsevier, 2015; pp. 85–101. <https://doi.org/10.1016/B978-1-78242-305-8.00005-X>.
48. John, S.K.; Cascardi, A.; Nadir, Y.; Aiello, M.A.; Girija, K. A New Artificial Neural Network Model for the Prediction of the Effect of Molar Ratios on Compressive Strength of Fly Ash-Slag Geopolymer Mortar. *Advances in Civil Engineering* **2021**, *2021*, 1–17, doi:10.1155/2021/6662347. <https://doi.org/10.1155/2021/6662347>.
49. Shirin, S.; Jamal, A.; Emmanouil, C.; Yadav, A.K. Assessment of Characteristics of Acid Mine Drainage Treated with Fly Ash. *Applied Sciences* **2021**, *11*, 3910, doi:10.3390/app11093910. <https://doi.org/10.3390/app11093910>.
50. Imkum Putkham, A.; Chuakham, S.; Chaiyachet, Y.; Suwansopa, T.; Putkham, A. Production of Bio-Calcium Oxide Derived from Hatchery Eggshell Waste Using an Industrial-Scale Car Bottom Furnace. *J Renew Mater* **2022**, *10*, 1137–1151, doi:10.32604/jrm.2022.018560. <https://doi.org/10.32604/jrm.2022.018560>.
51. Vanthana Sree, G.; Nagaraaj, P.; Kalanidhi, K.; Aswathy, C.A.; Rajasekaran, P. Calcium Oxide a Sustainable Photocatalyst Derived from Eggshell for Efficient Photo-Degradation of Organic Pollutants. *J Clean Prod* **2020**, *270*, 122294, doi:10.1016/j.jclepro.2020.122294. <https://doi.org/10.1016/j.jclepro.2020.122294>.
52. Yadav, V.K.; Yadav, K.K.; Cabral-Pinto, M.M.S.; Choudhary, N.; Gnanamoorthy, G.; Tirth, V.; Prasad, S.; Khan, A.H.; Islam, S.; Khan, N.A. The Processing of Calcium Rich Agricultural and Industrial Waste for Recovery of Calcium Carbonate and Calcium Oxide and Their Application for Environmental Cleanup: A Review. *Applied Sciences* **2021**, *11*, 4212, doi:10.3390/app11094212. <https://doi.org/10.3390/app11094212>.
53. Ajayan, N.; K. P, S.; A. U., A.; Soman, S. Quantitative Variation in Calcium Carbonate Content in Shell of Different Chicken and Duck Varieties. *Advances in Zoology and Botany* **2020**, *8*, 1–5, doi:10.13189/azb.2020.080101. <https://doi.org/10.13189/azb.2020.080101>.
54. Uddin, Md.R.; Khandaker, M.U.; Akter, N.; Ahmed, Md.F.; Hossain, S.Md.M.; Gafur, A.; Abedin, Md.J.; Rahman, Md.A.; Idris, A.M. Identification and Economic Potentiality of Mineral Sands Resources of Hatiya Island, Bangladesh. *Minerals* **2022**, *12*, 1436, doi:10.3390/min12111436. <https://doi.org/10.3390/min12111436>.
55. Chen, Y.-L.; Lin, C.-T. Recycling of Basic Oxygen Furnace Slag as a Raw Material for Autoclaved Aerated Concrete Production. *Sustainability* **2020**, *12*, 5896, doi:10.3390/su12155896. <https://doi.org/10.3390/su12155896>.
56. Dong, M.; Ruan, S.; Zhan, S.; Shen, S.; Sun, G.; Qian, X.; Zhou, X. Utilization of Red Mud with High Radiation for Preparation of Autoclaved Aerated Concrete (AAC): Performances and Microstructural Analysis. *J Clean Prod* **2022**, *347*, 131293, doi:10.1016/j.jclepro.2022.131293. <https://doi.org/10.1016/j.jclepro.2022.131293>.
57. Fudge, C.; Fouad, F.; Klingner, R. Autoclaved Aerated Concrete. In *Developments in the Formulation and Reinforcement of Concrete*; Elsevier, 2019; pp. 345–363. <https://doi.org/10.1016/B978-0-08-102616-8.00015-0>.
58. Agrawal, Y.; Gupta, T.; Siddique, S.; Sharma, R.K. Potential of Dolomite Industrial Waste as Construction Material: A Review. *Innovative Infrastructure Solutions* **2021**, *6*, 205, doi:10.1007/s41062-021-00570-5. <https://doi.org/10.1007/s41062-021-00570-5>.
59. Junaid, M.F.; Rehman, Z. ur; Kuruc, M.; Medved, I.; Bačinskas, D.; Čurpek, J.; Čekon, M.; Ijaz, N.; Ansari, W.S. Lightweight Concrete from a Perspective of Sustainable Reuse of Waste Byproducts. *Constr Build Mater* **2022**, *319*, 126061, doi:10.1016/j.conbuildmat.2021.126061. <https://doi.org/10.1016/j.conbuildmat.2021.126061>.
60. Shah, S.N.; Mo, K.H.; Yap, S.P.; Yang, J.; Ling, T.-C. Lightweight Foamed Concrete as a Promising Avenue for Incorporating Waste Materials: A Review. *Resour Conserv Recycl* **2021**, *164*, 105103, doi:10.1016/j.resconrec.2020.105103. <https://doi.org/10.1016/j.resconrec.2020.105103>.
61. Sundaralingam, K.; Peiris, A.; Anburuvel, A.; Sathiparan, N. Quarry Dust as River Sand Replacement in Cement Masonry Blocks: Effect on Mechanical and Durability Characteristics. *Materialia (Oxf)* **2022**, *21*, 101324, doi:10.1016/j.mtla.2022.101324. <https://doi.org/10.1016/j.mtla.2022.101324>.
62. Wang, S.; Yu, L.; Yang, F.; Zhang, W.; Xu, L.; Wu, K.; Tang, L.; Yang, Z. Resourceful Utilization of Quarry Tailings in the Preparation of Non-Sintered High-Strength Lightweight Aggregates. *Constr Build Mater* **2022**, *334*, 127444, doi:10.1016/j.conbuildmat.2022.127444. <https://doi.org/10.1016/j.conbuildmat.2022.127444>.

63. Addich, M.; El Baraka, N.; Laknifli, A.; Saffaj, N.; Fatni, A.; El Hammadi, A.; Alrashdi, A.A.; Lgaz, H. New Low-Cost Tubular Ceramic Microfiltration Membrane Based on Natural Sand for Tangential Urban Wastewater Treatment. *Journal of Saudi Chemical Society* **2022**, *26*, 101512, doi:10.1016/j.jscs.2022.101512. <https://doi.org/10.1016/j.jscs.2022.101512>.
64. Burduhos Nergis, D.D.; Abdullah, M.M.A.B.; Sandu, A.V.; Vizureanu, P. XRD and TG-DTA Study of New Alkali Activated Materials Based on Fly Ash with Sand and Glass Powder. *Materials* **2020**, *13*, 343, doi:10.3390/ma13020343. <https://doi.org/10.3390/ma13020343>.
65. Abubakar, M.; Muthuraja, A.; Rajak, D.K.; Ahmad, N.; Pruncu, C.I.; Lamberti, L.; Kumar, A. Influence of Firing Temperature on the Physical, Thermal and Microstructural Properties of Kankara Kaolin Clay: A Preliminary Investigation. *Materials* **2020**, *13*, 1872, doi:10.3390/ma13081872. <https://doi.org/10.3390/ma13081872>.
66. Nannoni, A.; Piccini, L.; Costagliola, P.; Batistoni, N.; Gabellini, P.; Cioni, R.; Pratesi, G.; Bucci, S. Innovative Approaches for the Sedimentological Characterization of Fine Natural and Anthropogenic Sediments in Karst Systems: The Case of the Apuan Alps (Central Italy). *Front Earth Sci (Lausanne)* **2021**, *9*, doi:10.3389/feart.2021.672962. <https://doi.org/10.3389/feart.2021.672962>.
67. Tchappa Gnamsi, G.M.; Mambou Ngueyep, L.L.; Foguieng Wembe, M.; Ndjaka, J.-M.B. Microstructure Analysis of Hydraulic Concrete Using Crushed Basalt, Crushed Gneiss and Alluvial Sand as Fine Aggregate. *JMST Advances* **2020**, *2*, 25–35, doi:10.1007/s42791-020-00031-7. <https://doi.org/10.1007/s42791-020-00031-7>.
68. Castro, L. da S.; Barañano, A.G.; Pinheiro, C.J.G.; Menini, L.; Pinheiro, P.F. Biodiesel Production from Cotton Oil Using Heterogeneous CaO Catalysts from Eggshells Prepared at Different Calcination Temperatures. *Green Processing and Synthesis* **2019**, *8*, 235–244, doi:10.1515/gps-2018-0076. <https://doi.org/10.1515/gps-2018-0076>.
69. Razali, N.; Jumadi, N.; Jalani, A.Y.; Kamarulzaman, N.Z.; Faizal, K.; Ee, P. Thermal Decomposition of Calcium Carbonate in Chicken Eggshells: Study on Temperature and Contact Time (*Penguraian Kalsium Karbonat Dalam Kulit Telur Ayam: Kajian Mengenai Suhu Dan Masa*); 2022; Vol. 26. https://mjas.analis.com.my/mjas/v26_n2/pdf/Nadia_26_2_14.pdf
70. Moreau, T.; Gautron, J.; Hincke, M.T.; Monget, P.; Réhault-Godbert, S.; Guyot, N. Antimicrobial Proteins and Peptides in Avian Eggshell: Structural Diversity and Potential Roles in Biomineralization. *Front Immunol* **2022**, *13*, doi:10.3389/fimmu.2022.946428. <https://doi.org/10.3389/fimmu.2022.946428>.
71. Jakfar, N.H.; Fhan, K.S.; Johar, B.; Shima Adzali, N.M.; Mohd. Yunus, S.N.H.; Meng, C.E. Crystal Structure and Thermal Behaviour of Calcium Monosilicate Derived from Calcined Chicken Eggshell and Rice Husk Ash. *J Phys Conf Ser* **2021**, *2129*, 012040, doi:10.1088/1742-6596/2129/1/012040. <https://doi.org/10.1088/1742-6596/2129/1/012040>.
72. Toibah, A.R.; Misran, F.; Shaaban, A.; Mustafa, Z. Effect of PH Condition during Hydrothermal Synthesis on the Properties of Hydroxyapatite from Eggshell Waste. *Journal of Mechanical Engineering and Sciences* **2019**, *13*, 4958–4969, doi:10.15282/jmes.13.2.2019.14.0411. <https://doi.org/10.15282/jmes.13.2.2019.14.0411>.
73. Saldanha, R.B.; da Rocha, C.G.; Caicedo, A.M.L.; Consoli, N.C. Technical and Environmental Performance of Eggshell Lime for Soil Stabilization. *Constr Build Mater* **2021**, *298*, 123648, doi:10.1016/j.conbuildmat.2021.123648. <https://doi.org/10.1016/j.conbuildmat.2021.123648>.
74. Consoli, N.C.; Caicedo, A.M.L.; Beck Saldanha, R.; Filho, H.C.S.; Acosta, C.J.M. Eggshell Produced Limes: Innovative Materials for Soil Stabilization. *Journal of Materials in Civil Engineering* **2020**, *32*, doi:10.1061/(ASCE)MT.1943-5533.0003418. [https://doi.org/10.1061/\(ASCE\)MT.1943-5533.0003418](https://doi.org/10.1061/(ASCE)MT.1943-5533.0003418).
75. Zhuang, S.; Wang, Q.; Zhang, M. Water Absorption Behaviour of Concrete: Novel Experimental Findings and Model Characterization. *Journal of Building Engineering* **2022**, *53*, 104602, doi:10.1016/j.job.2022.104602. <https://doi.org/10.1016/j.job.2022.104602>.
76. Kewalramani, M.; Khartabil, A. Porosity Evaluation of Concrete Containing Supplementary Cementitious Materials for Durability Assessment through Volume of Permeable Voids and Water Immersion Conditions. *Buildings* **2021**, *11*, 378, doi:10.3390/buildings11090378. <https://doi.org/10.3390/buildings11090378>.
77. Lamidi, Y.D.; Owoeye, S.S.; Abegunde, S.M. Preparation and Characterization of Synthetic Tobermorite (CaO–Al₂O₃–SiO₂–H₂O) Using Bio and Municipal Solid Wastes as Precursors by Solid State Reaction. *Boletín de la Sociedad Española de Cerámica y Vidrio* **2022**, *61*, 76–81, doi:10.1016/j.bsecv.2020.07.003. <https://doi.org/10.1016/j.bsecv.2020.07.003>.

78. Luo, S.; Jiang, Z.; Zhao, M.; Yang, L.; Castro-Gomes, J.; Wei, S.; Mi, T. Microwave Hydrothermal Synthesis of Tobermorite for the Solidification of Iron. *Case Studies in Construction Materials* **2023**, *19*, e02267, doi:10.1016/j.cscm.2023.e02267. <https://doi.org/10.1016/j.cscm.2023.e02267>.
79. Arif Kamal, M. Analysis of Autoclaved Aerated Concrete (AAC) Blocks with Reference to Its Potential and Sustainability. *Journal of Building Materials and Structures* **2020**, *7*, 76–86, doi:10.34118/jbms.v7i1.707. <https://doi.org/10.34118/jbms.v7i1.707>.
80. Ikechukwu, A.F.; Shabangu, C. Strength and Durability Performance of Masonry Bricks Produced with Crushed Glass and Melted PET Plastics. *Case Studies in Construction Materials* **2021**, *14*, e00542, doi:10.1016/j.cscm.2021.e00542. <https://doi.org/10.1016/j.cscm.2021.e00542>.
81. Dai, S.; Wen, Q.; Huang, F.; Bao, Y.; Xi, X.; Liao, Z.; Shi, J.; Ou, C.; Qin, J. Preparation and Application of MgO-Loaded Tobermorite to Simultaneously Remove Nitrogen and Phosphorus from Wastewater. *Chemical Engineering Journal* **2022**, *446*, 136809, doi:10.1016/j.cej.2022.136809. <https://doi.org/10.1016/j.cej.2022.136809>.
82. Qin, J.; Fang, Y.; Ou, C.; Wang, J.; Huang, F.; Wen, Q.; Liao, Z.; Shi, J. Highly Efficient Cd²⁺ and Cu²⁺ Removal by MgO-Modified Tobermorite in Aqueous Solutions. *J Environ Chem Eng* **2023**, *11*, 109534, doi:10.1016/j.jece.2023.109534. <https://doi.org/10.1016/j.jece.2023.109534>.
83. Yang, Z.; Fang, C.; Jiao, Y.; Zhang, D.; Kang, D.; Wang, K. Study on Crystal Growth of Tobermorite Synthesized by Calcium Silicate Slag and Silica Fume. *Materials* **2023**, *16*, 1288, doi:10.3390/ma16031288. <https://doi.org/10.3390/ma16031288>.

Disclaimer/Publisher's Note: The statements, opinions and data contained in all publications are solely those of the individual author(s) and contributor(s) and not of MDPI and/or the editor(s). MDPI and/or the editor(s) disclaim responsibility for any injury to people or property resulting from any ideas, methods, instructions or products referred to in the content.